Journal of Applied Polymer Science

Surface Coated Iron Particles via Atom Transfer Radical Polymerization for Thermal-Oxidatively Stable High Viscosity Magnetorheological Fluid

Joko Sutrisno,[1] Alan Fuchs,[1] Huseyin Sahin,[2] Faramarz Gordaninejad[2]
[1]Chemical Engineering Department, University of Nevada, Reno
[2]Mechanical Engineering Department, University of Nevada, Reno
Correspondence to: A. Fuchs (E-mail: afuchs@unr.edu)

ABSTRACT: A surface grafting technique for poly(2-fluorostyrene) onto iron particles via atom transfer radical polymerization (ATRP) is described. Grafted poly(2-fluorostyrene)–iron particles were synthesized by immobilizing 2-4(-chlorosulfonylphenyl)-ethyltrichlorosilane to the iron particles through the covalent bond of a silanol group, followed by the polymerization of 2-fluorostyrene monomer. The grafted polymer–iron particles display a higher thermal transition temperature compared to bulk polymer because the covalent bond between the polymer backbone and the surface of the iron particles restricts the molecular mobility. The molecular weight of the synthesized poly(2-fluorostyrene) has been measured and it has a narrow molecular weight distribution ($M_w/M_n <$ 1.1). From thermogravimetric analysis, the thermal stability of poly(2-fluorostyrene) is superior to polystyrene. Also, the high viscosity magnetorheological fluid (HVMRF) prepared from surface coated iron particles has excellent thermo–oxidative stability, having nearly constant viscosity. These materials exhibit a large increase in shear yield stress for the off- and on-state as compared to a benchmark high viscosity magnetorheological fluid (HVMRF) and -coated iron particle HVMRF. In addition, this type of fluid eliminates iron particle settling which is a common problem found in traditional magnetorheological fluids (MRFs). © 2012 Wiley Periodicals, Inc. J. Appl. Polym. Sci. 000: 000–000, 2012

KEYWORDS: surface grafting; poly(2-fluorostyrene); ATRP; magnetorheological fluid (MRF)

Received 28 April 2011; accepted 12 June 2012; published online
DOI: 10.1002/app.38199

INTRODUCTION

Atom transfer radical polymerization (ATRP) was introduced by Matyjaszewski's group[1] and was widely used to synthesize polymers that have controlled morphologies, functionality, and compositions. This polymerization technique involves an organic halide initiator, metal halides as a catalyst and a ligand to improve the solubility of the metal halides in the organic reaction system.[1,2] ATRP provides more flexibility in terms of the variety of monomers available. A wide range of monomers can be polymerized using ATRP either at mild conditions or elevated temperature. The polymers that have been synthesized using ATRP have a narrow polydispersity index due to the high ratio of dormant species to active species.[1–5]

The grafting technique of thermo-responsive poly(*N*-isopropylacrylamide) (poly(NIPAAm)) onto silica nanoparticles using ATRP has been investigated.[4,5] ATRP has been used for the polymerization of a series of substituted styrenes.[6] It has been shown that these polymers have polydispersities that are relatively low ($M_w/M_n < 1.5$). Surface polymerization of a block co-polymer of poly(styrene-*b*-methyl methacrylate) (PS-*b*-PMMA) and polystyrene (PS) with polydispersity index (PDI) of 1.29 on silica particles using ATRP has been investigated.[7] The properties of composite materials, such as magnetorheological fluids (MRFs) which consist of an inorganic substrate can be improved by introducing a polymer coating on the inorganic substrate. ATRP can be used as a tool to covalently graft various polymers onto the inorganic surface.

MRFs are intelligent, composite materials which have controllable rheological properties. MRFs consists of magnetic particles and a carrier fluid which is the dispersion medium for the magnetic particles. MRFs have excellent mechanical and rheological properties which can be controlled using an external magnetic field. MRFs also have properties similar to Newtonian fluids in the off-state condition (without magnetic field). Magnetic particles create chain-like structures within the MRF when external magnetic fields are applied and fluid flow is then restricted. This fluid-like material then transforms into a pseudo-solid material.

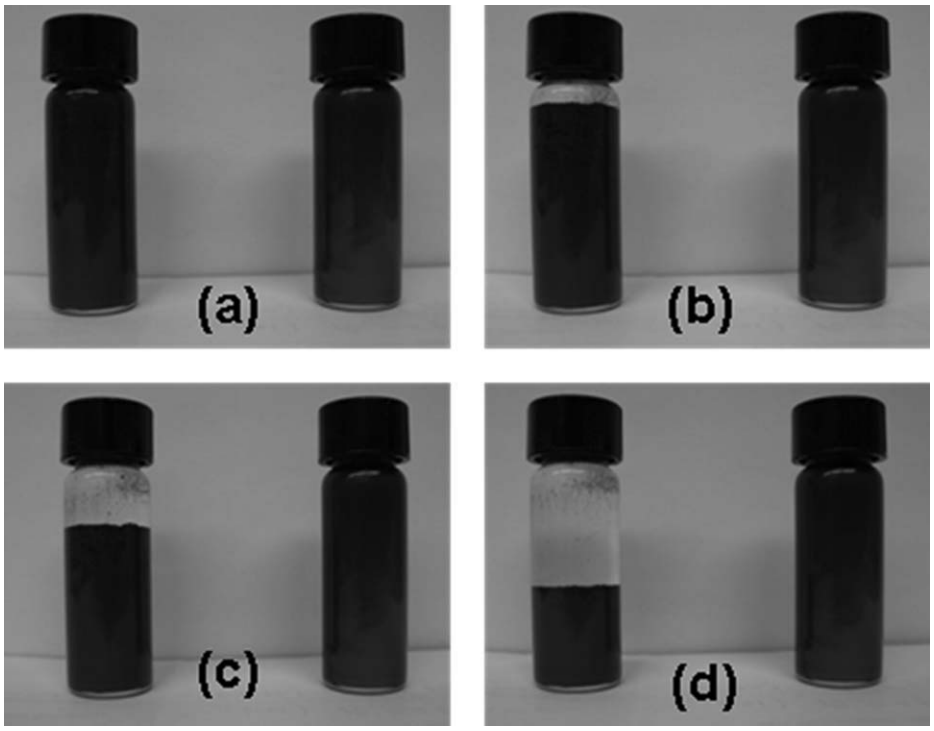

Figure 1. The settling behavior between MRF (left) and HVMRF (right) as function of elapsed time; (a) 0 min, (b) 1 min, (c) 3 min, and (d) 30 min.

Generally, a MRF consists of three different components: magnetic particles (iron), carrier fluid, and additives. Carrier fluids act to suspend the iron particles and other components, while additives serve as stabilizers and protect the iron particle surface. This provides a long operating life and prevents damage to devices which are used with these fluids. In addition, iron surface treatment prevents aggregation between the iron particles. MRF has several features including: low device abrasion, low settling, redispersibility, a wide range of operating temperatures (typically −50°C–150°C), chemical stability, high magnetic saturation, and excellent durability.

Preventing settling of iron particles in MRF is a challenge. There are several ways to reduce iron particle settling. By adding thickeners, settling of iron particles is reduced, resulting in a high viscosity magnetorheological fluid (HVMRF). Another way to reduce settling is by coating the iron surface using polymers. Surface coating decreases the density of the iron particles, and redispersion is accomplished easily. Even though particle settling takes place, only slight shearing is required to redisperse the iron particles in the carrier fluid. Fuchs et al.[8] has also investigated supramolecular polymers to coat iron particles using coordinated zinc terpyridine which offers better redispersion of iron particles. The settling behavior between MRF and HVMRF as a function of elapsed time is shown in Figure 1.

The carrier fluid in HVMRF plays an important role due to issues of chemical resistance, operating temperature range, viscosity, and vapor pressure. Mineral oil, poly(alfa olefins) (PAO), and silicone oil are common carrier fluids in HVMRF.[9] The thickeners used in most high viscosity fluids (HVFs) are made from metal-salt soaps, generally from one of the following types: "aluminum, aluminum complex, calcium, calcium complex, lithium, lithium complex, polyurea, and clay".[9] The cause of degradation in greases is the metal-salt soap catalyzed reaction between the hydrocarbons and oxygen. The oxidative stability of esters was improved through addition of phosphorus derivatives.[10] Improvement in the stability of magnetorheological fluids has been investigated using a viscoelastic medium that involves mixing vacuum grease and silicone oil as carrier fluids and magnetic nanoparticle additives ~ 30 nm in diameter (CrO_2 particles).[11] An oil-soluble cadmium dipropyldithiophosphate has been synthesized. The soft cadmium layer deposits played an important role in improving anti-wear and load carrying capability.[12] Four rare earth hexadecylate (La, Pr, Sm, Gd) complexes are used as additives in lithium HVF.

For engineering applications, Rabinow[13] investigated MR effects in the late 1940s. In the 1980s, MRFs were investigated extensively. Currently, several novel applications for HVMRFs are being explored—these include: shock absorbers, engine mounts, clutches, seat dampers, exercise equipment, and optical lenses.[14] The application of MRFs in the "fail-safe" damper devices for bicycle, motorcycle, and land vehicles has been investigated.[15]

In this work, grafting of poly(2-fluorostyrene) onto iron particles via ATRP polymerization and characterization are reported. HVMRF with excellent thermal and oxidative stability is synthesized from carrier fluids (such as polyalphaolefins, PAOs), magnetic particles (surface coated iron) and additives. The concentration of magnetic particles is 80 wt %. Poly(2-fluorostyrene) has a narrow polydispersity index which implies that the thickness of the surface coating on the iron particles is uniform. In addition, the viscoelastic properties of HVMRF,

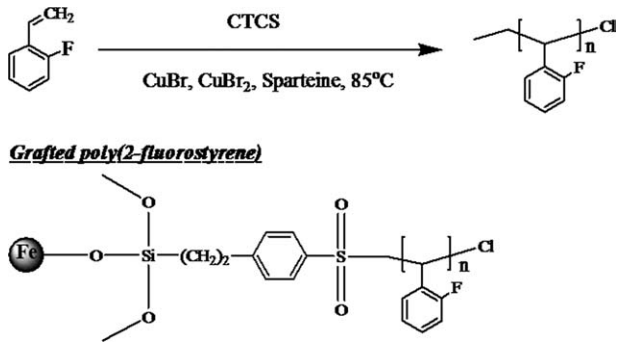

Figure 2. Synthesis of poly(2-fluorostyrene) via ATRP and surface grafted poly(2-fluorostyrene) on iron particles.

properties of the surface coated polymer, and the thermal–oxidative effect on the viscoelastic properties of HVMRF are characterized and compared to a benchmark HVMRF. To the best of our knowledge, this is the first time that surface coated iron particles using poly(2-fluorostyrene) have been used for HVMRF applications.

EXPERIMENTAL

Materials

The chemicals used in these studies were used as received. Carbonyl iron powder CN (3–7 μm, BASF), 2-fluorostyrene (Aldrich), methanol (Aldrich), ethanol (AAPER), 1-octyl-2-pyrrolidone (Aldrich), CuBr (Aldrich), $CuBr_2$ (Aldrich), sparteine (Aldrich), toluene (Aldrich), 2-4(-chlorosulfonylphenyl)-ethytrichlorosilane (CTCS) (Gelest Inc.), poly(alfa olefin) (PAO) (CP Chem), mineral oil (PTI Process Chemicals), sorbitan monooleate (Span 80) (Aldrich), modified smectite clay (Claytone), poly BD® R-45 HTLO (Sartomer company), PAPI 27 (Dow), stearic acid (Alfa Aesar), lithium hydroxide (Alfa Aesar), boric acid (Alfa Aesar), tris(nonylphenyl) phosphite (Aldrich).

Synthesis

ATRP of 2-Fluorostyrene for Iron Particles Surface Coating. The procedure for surface coating of iron particles using poly(2-fluorostyrene) via ATRP is as follows: 400 g of iron particles is washed with distilled water and then ethanol. Then, they are dried in a vacuum oven at 50°C and under nitrogen purge for 24 h and cooled down. Dried iron particles are added and reacted at 85°C with 6 g CTCS for 24 h under nitrogen with 110 g of toluene as a solvent. The mixture is filtered and washed with methanol in order to remove excess CTCS. The residual (Fe-CTCS) is dried in a vacuum oven at 40°C for 24 h. 2-fluorostyrene (monomer) 1.5 g, 120 g of functionalized Fe-CTCS are reacted with 0.1 g CuBr, 0.05 g $CuBr_2$, and 0.1 g spartein in 65 grams octyl pyrrolidone at 85°C in a four port reactor flask for 24 h under nitrogen. Finally, the mixture is filtered, washed several times with methanol, and dried in a vacuum oven at 40°C prior to use. Synthesis of poly(2-fluorostyrene) via ATRP and surface grafted poly(2-fluorostyrene) on iron particles is shown in Figure 2. The molecular weight of the surface grafted polymer is determined by reaction of a similar composition without the presence of iron particles. The poly(2-fluorostyrene) is isolated in acetone and washed several times.

Benchmark HVMRF. The benchmark HVMRF is synthesized based on the literature.[16] The iron particle content is maintained at 80 wt %. A HVF is prepared using mineral oil as the carrier fluid. Initially, mineral oil is added to a beaker that is equipped with mechanical stirring and a heating plate. The mineral oil is then heated up to 70°C, followed by gradually adding stearic acid until the oil is fully dissolved. The remaining chemicals: lithium hydroxide and boric acid are added slowly while being mixed at 200–500 rpm. The temperature of the mixing process is decreased to 40°C and the mixing process continues for 48 h. Benchmark HVMRF is synthesized by mixing lithium based HVF and pristine iron particles (80 wt %). The iron particles are added slowly to lithium-based HVF while stirred at 200 rpm until a uniform mixture is obtained. The composition of benchmark HVF is listed in Table I.

HVMRF. Two different types HVMRF were prepared: Type I (surface coated—HVMRF) was synthesized using surface coated iron particles/poly(2-fluorosyterene), and Type II (uncoated–HVMRF) was prepared using nonsurface-coated iron particles. Poly(alfa olefin) (PAO) was used as a carrier fluid for the HVMRF. The iron particle content was maintained at 80 wt %. First, the preparation of PAO-based HVF was performed as follows; PAO was weighed and a specified amount was added into a glass beaker equipped with a mechanical stirring and heating plate system. PAO was then heated up to 40°C and the ingredients were added (sorbitan monooleate, modified smectite clay, tris(nonylphenyl) phosphate, and liquid polyurethane) slowly. The mixture was stirred at 200–500 rpm until a homogenous mixture was obtained. Liquid polyurethane was prepared by reacting hydrocarbon polyol (Poly BD® R-45 HTLO) and polymeric MDI isocyanate (Dow PAPI 27). The weight ratio of polyol to isocyanate was 8.4–1. Second, HVMRF preparation was as follows: uncoated and coated iron particles/poly(2-fluorostyrene) were added to PAO based HVF until 80 wt % HVMRF was obtained, followed by mixing until the HVMRF mixture was uniform. The composition of HVMRF Type I (coated) and Type II (uncoated) is listed in Table II.

Characterization

Thermo-Oxidation Study. A thermo-oxidative study of HVMRF was performed to accelerate the oxidation and degradation of the HVMRF components at high temperature and pressure. The HVMRF was oxidized using a high pressure and high temperature stainless steel reactor equipped with inlet and outlet gas ports, thermometer port, and pressure gauge. The

Table I. Composition of Benchmark HVF[15]

Component	Weight %
Mineral oil	79.6
Lithium hydroxide, LiOH · H2O	3.8
Boric acid, H_3BO_3	2.4
Stearic acid, $CH_3(CH2)_{16}CO_2H$	14.2

Applied Polymer SCIENCE

Table II. Composition of HVMRF

Component	Weight % Type I	Weight % Type II	Role
PAO	16.33	16.33	Carrier fluid
Sorbitan monooleate	2.04	2.04	Dispersant
Modified smectite clay	1.02	1.02	Thickener[9]
Tris(nonylphenyl) phosphate	0.41	0.41	Anti-oxidant[9]
Polyurethane	0.20	0.20	Thickener
Iron particles	80.00 (iron + coating)	80.00 (iron only)	Magnetic particles

samples were placed in petri dishes and inserted on the aluminum rack within the reactor. The thermo-oxidation study conditions were set at 70–80°C and 50 psi of pressurized air for 48 h.[17–19]

Fourier Transform Infrared (FT-IR) Spectroscopy. The grafted poly(2-fluorostyrene)/iron particles were characterized using a Perkin-Elmer Spectrum 100 FTIR spectrometer. The grafted poly(2-fluorostyrene)/iron particles were dried in a vacuum oven at 60°C for 24 h and stored in a desiccator prior to characterization. The following samples were prepared: grafted poly(2-fluorostyrene)/iron particles (Fe–CTCS–poly(2-fluorostyrene)), immobilized surface initiator iron particles (Fe–CTCS), and uncoated iron (Fe). The samples were uniformly mixed with KBr powder at a weight ratio of 1 : 50, before mechanically pressing them to form moisture-free KBr pellets. All samples were scanned from 4000–400 cm^{-1} at room temperature.

Gel Permeation Chromatography. The molecular weight of poly(2-fluorostyrene) was characterized using a Shimadzu DGU-20A_3 degasser, LC-20AD pump, CTO-20AC column oven, RID-10A refractive index detector, CBM-20A controller, and single Phenogel 5 μm 10^4 angstrom column which has an effective molecular weight of 5000–500,000 g/mol. The mobile phase was *N,N*-dimethylformamide 99.9% HPLC grade with a flow rate of 1 mL/min, column temperature was set at 35°C, and 20 μL of polymer solution was injected through column. A calibration curve was generated with nearly monodisperse polystyrene standards purchased from Sigma Aldrich (certified by Scientific Polymer Product). Molecular weight averages and polydispersity index (M_w/M_n) of the polymer was calculated against polystyrene standards by using LabSolutions software.

Thermogravimetric Analysis. The thermal stability of the poly(2-fluorostyrene) and polystyrene were analyzed by Perkin-Elmer STA6000 thermogravimetric analysis (TGA). The analysis was performed on samples in a nitrogen atmosphere with a flow rate of 20 mL/min. Initially, the sample was held at a temperature of 30°C for 5 min, followed by scanning the sample at a rate of 10°C/min from 30°C to 700°C, and held at 700°C for 5 min.

Scanning Electron Microscopy – X-ray Energy Dispersive Spectrum (SEM-XEDS). The surface morphologies of grafted poly(2-fluorostyrene)/iron particles and chemical analysis of surface grafted poly(2-fluorostyrene)/iron particles were characterized using scanning electon micrcrosopy—X-ray energy dispersive spectroscopy (SEM-XEDS) with a Hitachi S-4700 equipped with an Oxford EDS System at magnifications from 400X to 15,000X at an accelerating potential of 20kV. EDS microanalysis was performed on the samples at magnifications ranging from 3000X to 15,000X and an accelerating potential of 20 kV. SEM samples were prepared by placing surface grafted poly(2-fluorostyrene)/iron particles onto carbon tapes adhered to an aluminum SEM sample holder. The mounted surface grafted poly(2-fluorostyrene)/iron particles samples were then coated with a thin layer of platinum using an argon plasma sputtering system. The platinum coating was done at an approximate rate of 25–30 nm/min with 85 mA. The number of atomic carbon after surface polymerization of poly(2-fluorostyrene) is expected to increase as compared with uncoated iron particles. Also, the presence of fluorine atoms provides evidence of the presence of poly(2-fluorostyrene) on the iron particles surfaces.

Differential Scanning Calorimetry. The thermal properties of the grafted poly(2-fluorostyrene) on the iron particles surfaces were characterized using Perkin-Elmer Pyris-1 DSC. Two pans placed in the DSC, one containing the sample and the other holding a reference sample. The grafted poly(2-fluorostyrene)/iron particles were dried in a vacuum oven at 60°C for 24 h and were stored in a desiccator prior to characterization. 17.3 mg of poly(2-fluorostyrene)/iron particles were placed in the sample pan and scanned from 50 to 350°C with a heating rate of 10°C/min under a high purity nitrogen purge with a volumetric flow rate of 20 mL/min.

Rheological Measurements. The rheological properties of HVMRF, viscosity, and shear stress, were investigated using a parallel-plate MR fluid rheometer (Paar Physica model MCR 300 and MRD180). For this study, parallel plates with a diameter of 20 mm were used to obtain rheological properties of HVMRF under the application of a magnetic field (on-state; 0.282Tesla and 0.529Tesla). The MR rotational rheometer could provide absolute quantitative measurements of viscosity and viscoelasticity of HVMRF samples at a range of temperatures from 10 to 80°C. A sample volume of $\sim$ 0.315 mL was filled in a constant gap of 1.0 mm between two parallel plates during the experiment. Results obtained have a possible error of $\pm$0.05 mL due to the difficulty in filling the gap with HVMRF. A constant shear rate over the range of 1–400 s^{-1} was applied, and shear stress and shear viscosity were obtained and plotted. In addition, the MR fluid rheometer system was equipped with an MR cell having a parallel-plate configuration.

MCR 300 has a JULABO F25 temperature control unit equipped with a circulator head and a cooling machine with a bath tank, and it has been designed for heating and cooling of liquids in the bath tank. An electronic proportional temperature controller regulates the heat supplied to the bath. The rheology study was carried out for temperatures of 20 and 60°C (for off-

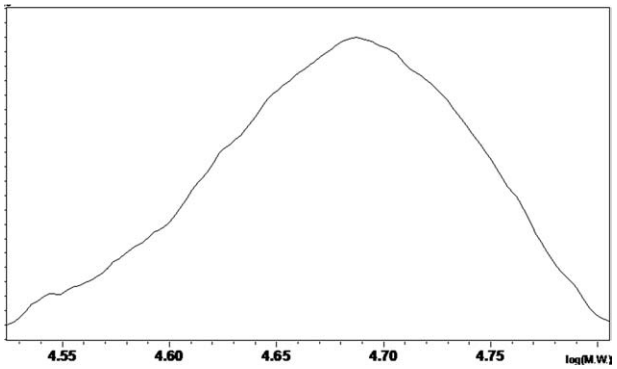

Figure 3. Molecular weight distribution of poly(2-fluorostyrene).

state) with an accuracy of ±0.01°C in the measurements. Error analysis of the experiment, 95% confidence interval (CI) was used, and was performed based on three experimental measurements for data taken (each achieved value at 400 s^{-1} of shear rate for viscosity and each value of extrapolated data for shear stress at 0 s^{-1} of shear rate for shear stress).

RESULTS AND DISCUSSION

Fourier Transform Infrared Spectroscopy

The comparison of the FTIR spectra of iron particles, immobilized surface initiator on the iron particles, and grafted poly(2-fluorostyrene)–iron particles were investigated and shown in the literature.[20] The hydroxyl stretch was shown by a peak at 3500–3400 cm^{-1}.[21,22] The double bond (C=C) stretch of the benzene ring of surface initiator and poly(2-fluorostyrene) was shown in the range of 1650–1600 cm^{-1} (Refs. 21,23,24) and the peak shift at 2950–2850 cm^{-1} (Ref. 25) was caused by the C—H bond stretching and bending of the surface initiator. In addition, the presence of the surface initiator and grafted poly(2-fluorostyrene) was also confirmed by the presence of a C—F and SO_2 stretching bond and a C—Cl bond which occurred at peaks at 1000–1250 cm^{-1} (Refs. 21,24,26), and 800–600 cm^{-1} (Refs. 21,24,25), respectively. It can be concluded that the poly(2-fluorostyrene) was successfully covalently bonded on the surface of the iron particles using a silane-based surface initiator by comparing the three infrared spectra.

Gel Permeation Chromatography

The GPC analysis shows that the polydispersity index (PDI) of poly(2-fluorostyrene) was narrow ($M_w/M_n < 1.1$), and the weight average molecular weight was 48,400. The addition of Cu-(II) bromide resulted in a narrow molecular weight distribution of polymer because it acted as a deactivator which led to the reduction of the growing chain rate (converting the propagating polymer chain into the dormant species) and reduction of the polymerization rate. In addition, the long polymerization time and the high temperature of the reaction allowed most of the monomer to be converted to polymer and it led to the narrow PDI.[1,27,28] The molecular weight distribution of poly(2-fluorostyrene) is shown in Figure 3.

Thermogravimetric Analysis

TGA of the polystyrene and poly(2-fluorostyrene) was measured in order to demonstrate that the thermal stability of poly(2-fluorostyrene) was higher than polystyrene. This is shown in Figure 4. The residual weight of polystyrene decreased drastically as compared with poly(2-fluorostyrene) in the temperature range between 350 and 450°C. Poly(2-fluorstyrene) underwent two different degradation stages. The first degradation took place in the temperature range of 300–400°C which may have been related to the degradation of the silane compounds from the organic initiator.[29] The second degradation (which was slower) took place in the temperature range of 400–700°C in which the fluorinated aromatic ring and polymer backbone bonds were broken. The fluorine atom on the benzene ring may decrease the degradation rate because the C—F bond reduces the structures overall energy and the bond is chemically inert as compared with polystyrene.[29,30] This results in higher stability of the polymer. The 50% residual weight ($T_{50\%}$) for polystyrene and poly(2-fluorostyrene) is shown at approximate temperatures of 400 and 545°C. At 600°C, the residual weight percentage of poly(2-fluorostyrene) still remained at 40 wt %.

Scanning Electron Microscopy—X-Ray Energy Dispersive Spectrum (SEM-XEDS)

ATRP is a controlled living polymerization which has significant advantages as compared with the regular radical polymerization process because the polymer is covalently bonded on the iron surface through a surface initiator (which is silane based), and uniform molecular weight of the polymer results.[1–5,31] This results in a uniform coating thickness on the particles surfaces. Also, another advantage of ATRP is controllable polymer architecture.[1–5] In this work, surface coating of the iron particles resulted in uniform "hairy" like polymer architecture. The "hairy" like surfaces of the coated iron particles and the spherical shape of the iron particles was maintained as is shown in the SEM images. The SEM images of non- and surface-coated iron particles are shown in Figure 5.

The presence of fluorine atoms on the polymer backbone of grafted poly(2-fluorostyrene)–iron particles is confirmed by quantitative elemental analysis which is recorded by x-ray energy dispersive spectroscopy. The samples are platinum sputter coated prior to observation. This platinum coating prevents

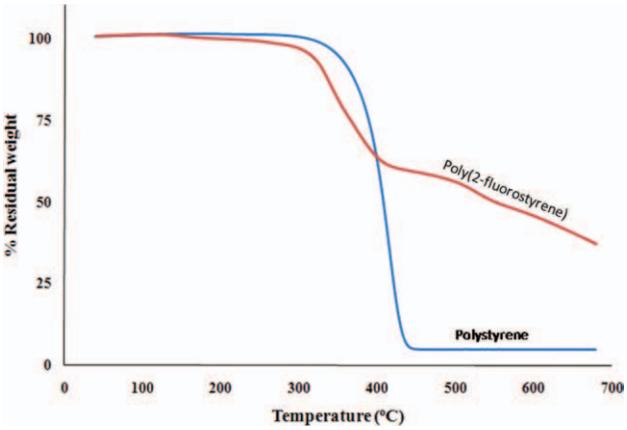

Figure 4. TGA weight loss profiles of poly(2-fluorostyrene) and polystyrene. [Color figure can be viewed in the online issue, which is available at wileyonlinelibrary.com.]

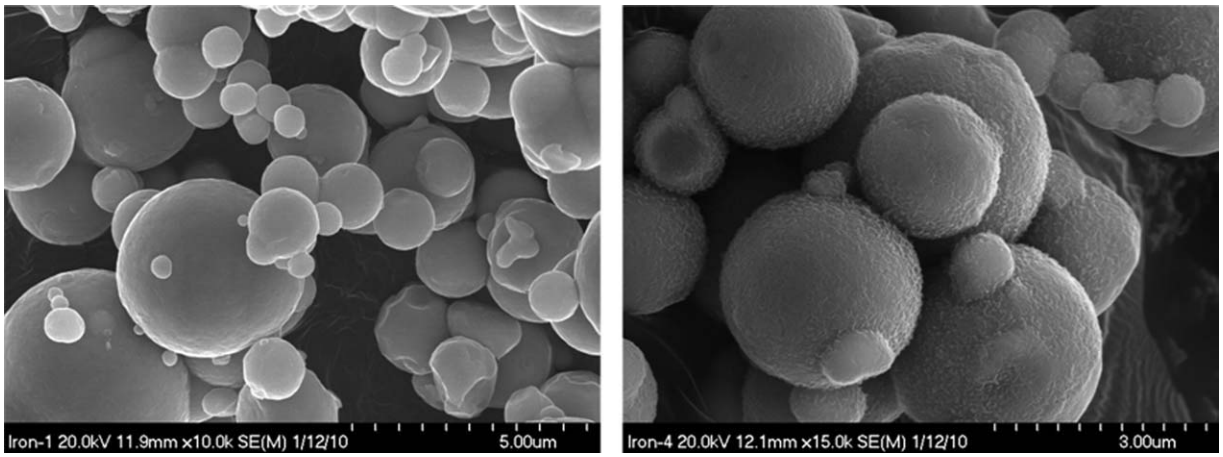

Figure 5. SEM images of non- and surface-coated iron particles.

the charging of the organic compound, distributes the effects of heating, and increases the intensity of secondary and back-scattered electrons at high resolution. Appropriate selection of the electron beam acceleration voltage is required to avoid thermal degradation of the sample, especially organic material, and to achieve accurate elemental quantification. The electron beam acceleration voltage used during this observation is 15 keV. During the scanning process, x-ray peaks are generated and used to record the elements that existed on the iron and surface modified particles. The elemental maps for the identified elements are also generated automatically during the scanning time. The electron beams are only able to penetrate a few nanometers deep into the sample surface. Because of this limitation, X–EDS analysis is used only to determine the presence of the grafted poly(2-fluorostyrene) on the iron particles. The X–EDS spectrograms are shown in Figure 6. The number of carbon atoms increase from pristine iron particles to the grafted poly(2-fluorostyrene)–iron particles. These results confirm that the polymerization of poly(2-fluorostyrene) on the iron particles has occurred. The presence of polymer on the particle surface is also supported by measurement of the weight fraction of iron particles after surface grafting of poly(2-fluorostyrene). The weight fraction of iron decreases after coating. This means that the iron particle is covered with the poly(2-fluorostyrene) coating. The weight percentage of each element for pristine iron particles, and the grafted poly(2-fluorostyrene) on the surface of iron particles from x-ray energy dispersive spectrograms is listed in Table III.

Differential Scanning Calorimetry

The glass transition temperature (T_g) of grafted polymer on the surface of iron particles is characterized using differential scanning calorimetry (DSC). The grafted poly(2-fluorostyrene)–iron particles have a glass transition temperature of 160.5°C and another thermal transition at 221.8°C. For comparison, pristine iron particles are scanned at the same temperature and no thermal transition resulted. In addition, grafted poly(2-fluorostyrene)–iron particles synthesized in our laboratory have a higher thermal transition temperature than grafted polystyrene on a silica surface, which has a thermal transition temperature of 133°C.[32] From the reported literature, the bulk polystyrene and poly(2-fluorostyrene) have glass transition temperatures of 102[32] and 96°C,[33] respectively. The higher thermal transition temperature for the grafted polymer is due to the covalently bonded polymer on the surface through the silanol group that restricts the mobility of the molecules.[32] As a result, additional energy is required to achieve the rubbery state of the grafted polymer. The DSC thermogram of iron particles and grafted poly(2-fluorostyrene)–iron particles is shown in Figure 7.

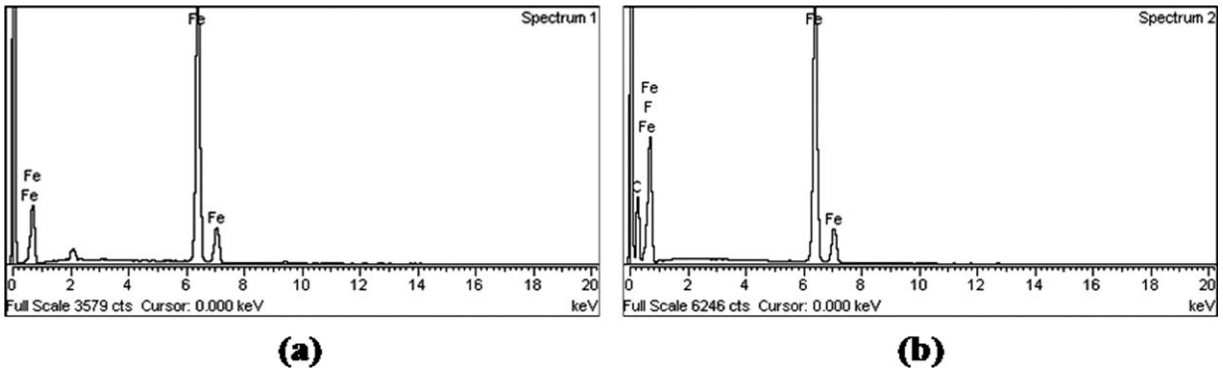

Figure 6. Energy dispersive X-ray analysis of; (a) Uncoated iron particles, and (b) The grafted poly(2-fluorostyrene) on the surface of iron particles.

Table III. Element Analysis from X-Ray Energy Dispersive (X–EDS)

	Weight %	
Element	Uncoated iron	Fe - poly(2-fluorostyrene)
Fe	100.00	61.48
C	0.00	37.04
F	0.00	1.48
Total	100.00	100.00

Rheological Measurements

HVMRF of composite magnetic iron particles at a concentration of 80 wt % in oils is prepared, and the rheological properties under various temperatures are investigated. Shear viscosity and shear stress is plotted as a function of shear rate up to 400 s^{-1}. Figure 8(a) demonstrates the dependency of HVMRF's shear viscosity and shear stress on temperature for off–state (without applied magnetic field). From HVMRF shear stress–shear rate behavior, it can be seen that shear stress (τ) is not a linear function of shear rate ($\dot{\gamma}$). This is shown in Figures 8(b) and 9(b). These HVMRF rheology data tend to follow the Bingham model. In addition, from the figures showing the HVMRF shear viscosity–shear rate, HVMRF has shear thinning behavior which is represented by decreasing shear viscosity values as the shear rate increases. According to the Bingham model, the yield stress of MRF can be found by extrapolating the shear stress curve at zero shear rates. For instance, from Figure 8(b), at an experimental temperature of 20°C and magnetic flux of 0 Tesla, the yield stress of MRF is nearly 369 Pa (±2%). In general, when the shear stress is smaller than the yield stress, the HVMRF behaves like a solid. On the other hand, HVMRF begins to flow when the applied shear stress is greater than the yield stress. This behavior has also been reported for MRF and electrorheological (ER) fluids.[34–37] The experiment is carried out at three different temperatures; 20, 40, and 60°C. Both shear viscosity and shear stress of HVMRF decrease significantly with increasing temperature, which is in agreement with the results previously reported in the literature.[37,38] The Bingham model is expressed as follow:[39,40]

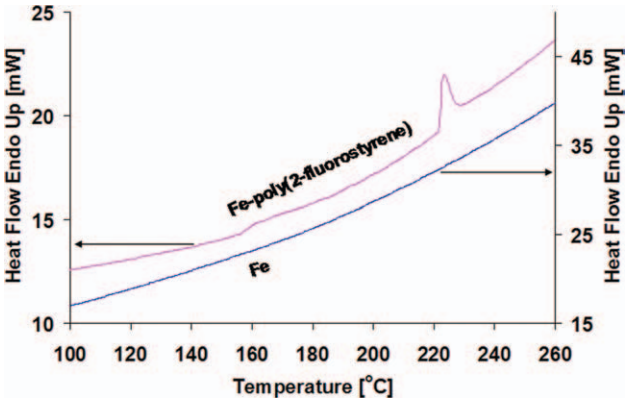

Figure 7. The DSC thermogram of iron and grafted poly(2-fluorostyrene)–iron particles. [Color figure can be viewed in the online issue, which is available at wileyonlinelibrary.com.]

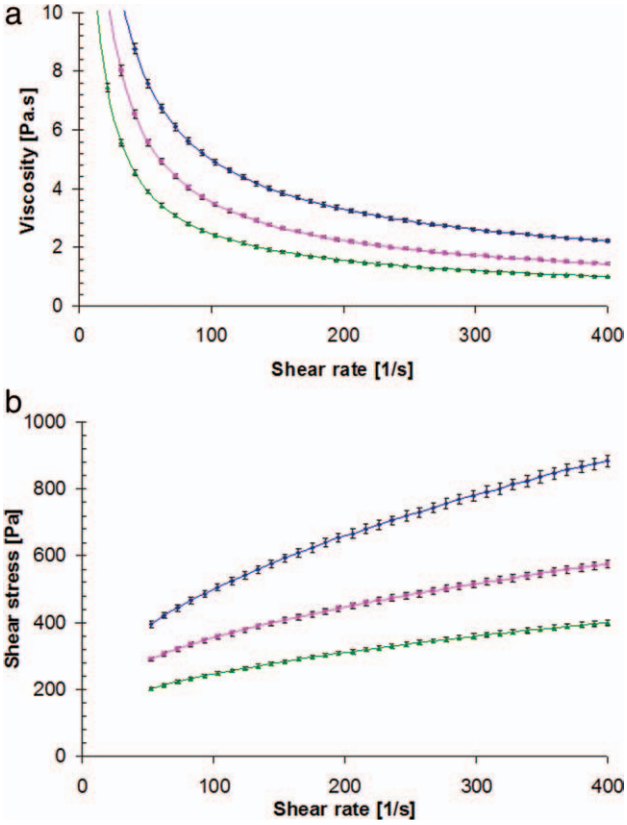

Figure 8. (a) Benchmark HVMRF shear viscosity as function of shear rate (off–state; 0 Tesla) at different temperature of 20°C (blue), 40°C (pink), and 60°C (green). (b) Benchmark HVMRF shear stress as function of shear rate (off–state; 0 Tesla) at different temperature of 20°C (blue), 40°C (pink), and 60°C (green). [Color figure can be viewed in the online issue, which is available at wileyonlinelibrary.com.]

$$\tau = \tau_y + \eta_0 \dot{\gamma}$$

where:

- τ is shear stress of HVMRF.
- τ_y is yield stress of HVMRF.
- η_0 is the viscosity at off–state.
- $\dot{\gamma}$ is shear rate.

The dependency of HVMRF's shear viscosity and shear stress on the temperature are also investigated for the on–state (with applied magnetic field, 0.282 Tesla). Figure 9(a,b) demonstrate similar HVMRF rheological properties (shear viscosity and shear stress) behavior at the off–state conditions when it was characterized at different temperatures; 20, 40, and 60°C. When shear viscosity and shear stress are plotted as a function of shear rate up to 400 s^{-1}, the results show both shear viscosity and shear stress of HVMRF decrease significantly with increasing temperature, which is also in agreement with results previously reported in the literature.[37] As a comparison, the shear viscosity values of HVMRF Type 1 (coated) at 20, 40, and 60°C (0.282Tesla and

Applied Polymer SCIENCE

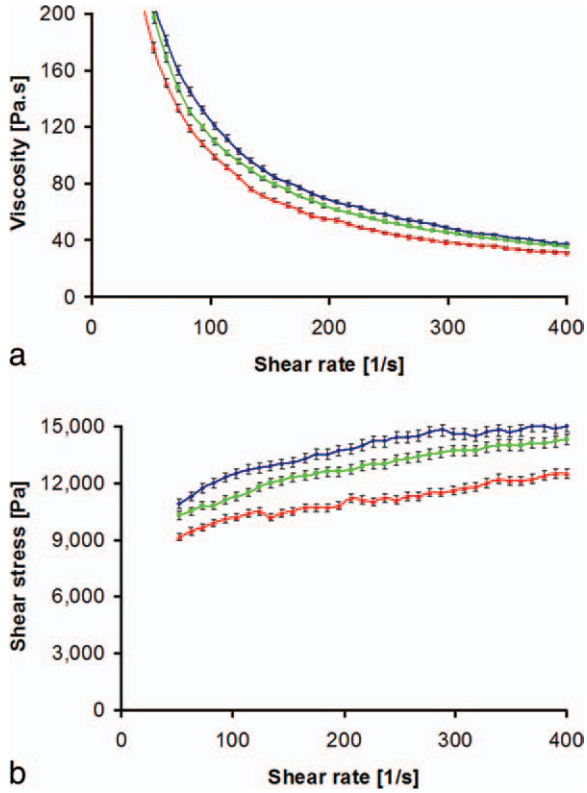

Figure 9. (a) HVMRF Type 1 shear viscosity as function of shear rate (on–state; 0.282 Tesla) at different temperature of 20°C (blue), 40°C (green), and 60°C (red). (b) HVMRF Type 1 shear stress as function of shear rate (on–state; 0.282 Tesla) at different temperature of 20°C (blue), 40°C (green), and 60°C (red). [Color figure can be viewed in the online issue, which is available at wileyonlinelibrary.com.]

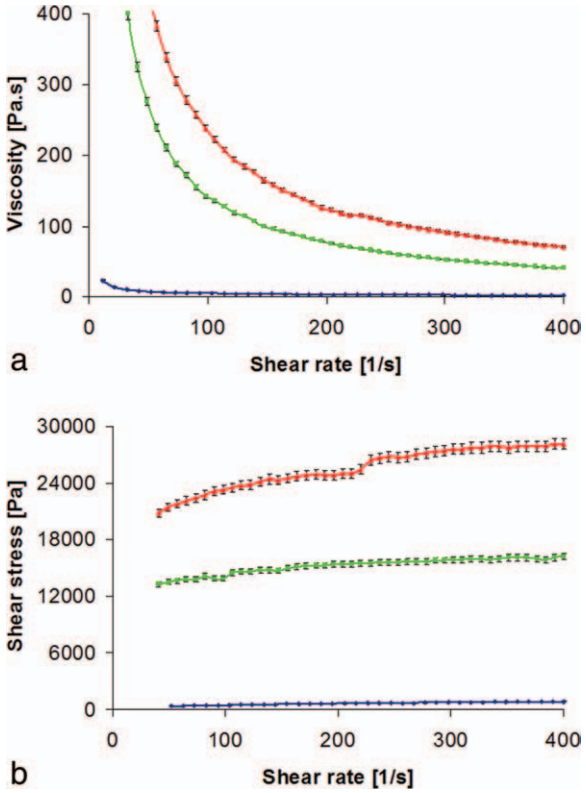

Figure 10. (a) Benchmark HVMRF shear viscosity as function of shear rate at 20°C with different applied magnetic field of 0 Tesla, 0.282 Tesla, and 0.529 Tesla. (b) Benchmark HVMRF shear stress as function of shear rate at 20°C with different applied magnetic field of 0 Tesla, 0.282 Tesla, and 0.529 Tesla. [Color figure can be viewed in the online issue, which is available at wileyonlinelibrary.com.]

400 s^{-1}) are 37.5 Pa s, 35.7 Pa s, and 31.3 Pa s (±2%), respectively. Also, the shear stress values of HVMRF Type 1 (coated) at 20, 40, and 60°C (0.282 Tesla and 400 s^{-1}) are 11.4 kPa, 10.3 kPa, and 9.2 kPa (±2%), respectively. The approximate change of HVMRF rheological properties is 20–25% from 20 to 60°C.

HVMRF of composite magnetic iron particles with a concentration of 80 wt % in oil was prepared, and the rheological properties under various applied magnetic fields (0 Tesla, 0.282 Tesla, and 0.529 Tesla) is investigated and illustrated in Figure 10(a,b). The rheological properties of all HVMRFs change drastically when it is exposed to magnetic fields. The yield stress of HVMRFs increases as the magnetic density is increased by applying higher magnetic fields, exhibiting distinguishable MR effects. As is expected, the MR effect is proportional to the applied magnetic field because the application of higher magnetic fields resulted in higher magnetic forces between iron particles in the HVMRFs. The rheological properties investigated in this work show reproducible results and are very consistent because of the spherical shape and high purity of the iron particles used. Similarly, the shear viscosity of HVMRF increases with increasing applied magnetic fields. The MR effect is calculated using the following equation:

$$\text{MR Effect} = \frac{\tau_{y\_on} - \tau_{y\_off}}{\tau_{y\_off}}$$

Where τ_{y_on} is yield stress of HVMRF at on–state and τ_{y_off} is yield stress of HVMRF at off–state. From Table IV, the MR effect of HVMRFs, Type I (coated) and Type II (uncoated), are higher than the benchmark HVMRF because the off–state yield stress of HVMRFs is lower than the benchmark. In addition, by comparing HVMRF Type I (coated) and Type II (uncoated), it can be concluded that surface-coated iron particles in HVMRF Type I (coated) decrease the MR Effect because the grafted poly(2-fluorostyrene) is not magnetizable and it reduces the magnetic permeability of the iron particles.

Table IV. The Summary of HVMRF MR Effect

Magnetic field [Tesla]	HVMRF shear stress [Pa] (± 2%) and MR effect (times)		
	Benchmark	Type I	Type II
0	369 (1x)	28 (1x)	42 (1x)
0.282	13,611 (36x)	11,385 (402x)	12,543 (298x)
0.529	22,608 (60x)	20,380 (720x)	21,262 (506x)

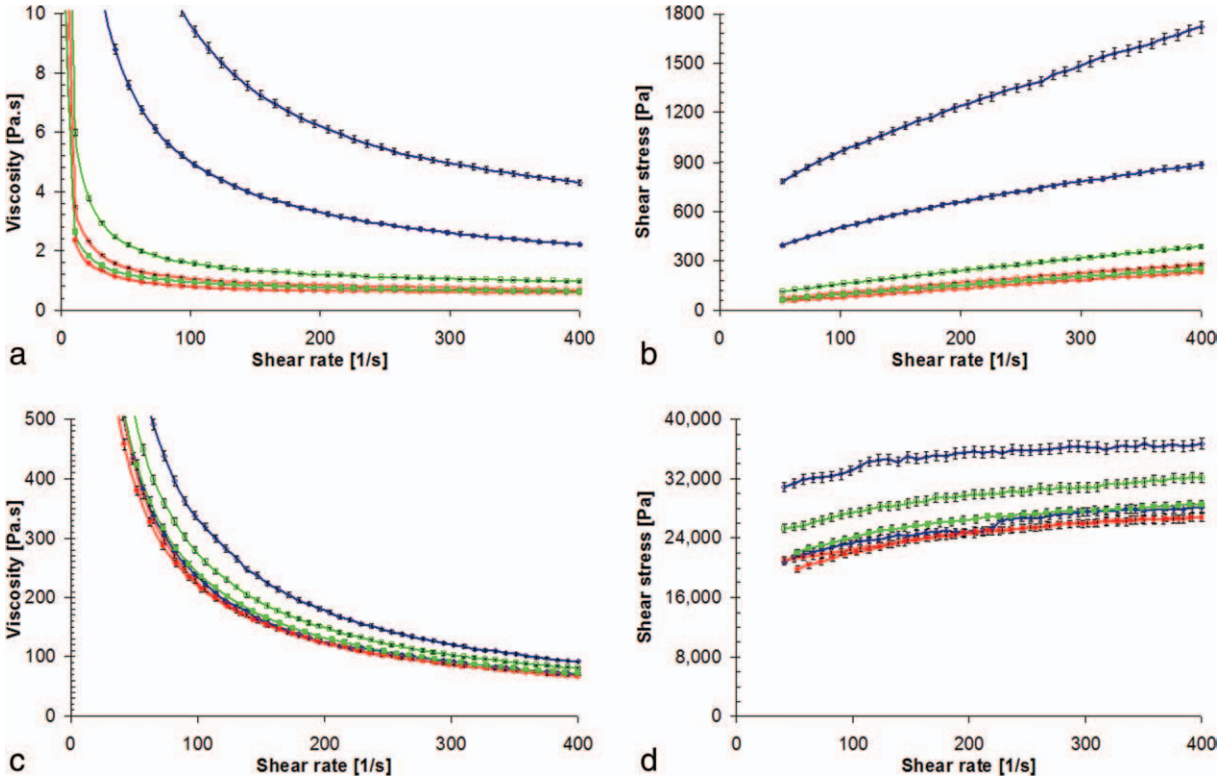

Figure 11. (a) The oxidation effect on HVMRF viscosity at off–state (0Tesla) for: Type I (red); Type II (green); and Benchmark (blue) (before–color filled; after–color blank). (b) The oxidation effect on HVMRF shear stress at off–state (0 Tesla) for: Type I (red); Type II (green); and Benchmark (blue) (before–color filled; after–color blank). (c) The oxidation effect on HVMRF viscosity at on–state (0.529 Tesla) for: Type I (red); Type II (green); and Benchmark (blue) (before–color filled; after–color blank). (d) The oxidation effect on HVMRF shear stress at on–state (0.529 Tesla) for: Type I (red); Type II (green); and Benchmark (blue) (before–color filled; after–color blank). [Color figure can be viewed in the online issue, which is available at wileyonlinelibrary.com.]

Figure 11(a–d) shows the effect of oxidation testing on the rheological properties of HVMRF. HVMRFs Type I (coated) exhibit higher consistency in rheology properties than Type II (uncoated) after the oxidation test. However, the shear stress and shear viscosity of benchmark HVMRF change significantly. The thermo-oxidative stability of HVMRF is related to the carrier fluid, polyalphaolefin, which has a higher boiling point than mineral oil. In addition, the additives of HVMRFs, such as phosphate based antioxidant,[10] and surface coating of iron particles using poly(2-fluorostyrene) contribute to the HVMRF's oxidative stability. At the off–state and 400 s^{-1} shear rate, the shear viscosity of the benchmark HVMRF before and after the oxidation test increased by a factor of 1.9. On the other hand, the HVMRF Type I (coated) and Type II (uncoated) increased by a factor of 1.2 and 1.5, respectively. This demonstrates that the HVMRFs Type I is less subject to oxidative degradation than the Type II.

Surface grafted poly(2-fluorostyrene) on the surface of iron particles helped to maintain the thermo-oxidative stability of HVMRF Type I (coated). Poly(2-fluorostyrene) has unique properties which result from the contribution of fluorine atoms which have a high electronegative nature and are strongly electron–withdrawing. The presence of the fluorine provides greater thermo-oxidative stability to the poly(2-fluorostyrene) coating.[29,41–44] The summary of the shear viscosity of HVMRFs before and after oxidation testing at 400 s^{-1} and 20°C is listed in Table V.

Table V. The Change of Shear Viscosity (Pa s) Before and After Oxidation Test at 400 s^{-1} and 20°C

	Benchmark			Type I			Type II		
Magnetic flux [Tesla]	Before	After	% Change	Before	After	% Change	Before	After	% Change
0	2.21	4.30	94.57	0.58	0.69	18.97	0.63	0.97	53.97
0.282	40.40	47.90	18.56	37.50	38.30	2.13	43.40	48.10	10.83
0.529	70.40	91.60	30.11	66.90	67.00	0.15	71.30	80.30	12.62

CONCLUSIONS

Thermo-oxidatively stable HVMRFs were prepared by mixing iron particles, carrier fluid, thickener, and additives. This approach results in elimination of the settling of iron particles in the fluids. Rheology data indicate that HVMRF tends to follow the Bingham model and has shear thinning behavior. The shear viscosity of HVMRF Type I (surface coated iron particles) insignificant change before and after oxidation at 37.50 Pa s (at magnetic flux of 0.282 T and 20°C). These rheology data suggest that HVMRF contain surface-coated iron particles have less effect from oxidation process in compare with noncoated iron particles. The surface of iron particles were coated by using poly(2-fluorostyrene) via the atom transfer radical polymerization (ATRP) grafting technique. Differential Scanning Calorimetry (DSC) data indicates that poly(2-fluorostyrene) has a glass transition temperature of 160.5°C which is suitable for a high temperature coating application because the fluorine present on the benzene ring reduces the degradation rate of the coating and because C—F decreases the structure overall energy and is more chemically inert. Also, The grafted poly(2-fluorostyrene)–iron particles have a higher thermal transition temperature as compared to bulk polymer because of the covalent bond between the polymer backbone and the iron particles surface. The presence of the silanol group restricts the molecules mobility.

ACKNOWLEDGMENTS

This project has been funded by National Science Foundation (NSF). Dr. Ravi Subramanian, Chemical and Materials Engineering Dept., University of Nevada, Reno, provided FTIR and TGA analysis. Dr. Mo Ahmadian, Chemical and Materials Engineering Dept.,University of Nevada, Reno, provided SEM–XEDS analysis.

REFERENCES

1. Matyjaszewski, K.; Xia, J. *Chem. Rev.* **2001,** *101*, 2921.
2. Odian, G. Principles of Polymerization, 4th ed.; New York: Wiley, **2004.**
3. Kamigaito, M.; Ando, T.; Sawamoto, M. *Chem. Rev.* **2001,** *101*, 3689.
4. Wu, T.; Zhang, Y.; Wang, X.; Liu, S. *Chem. Mater.* **2008,** *20*, 101.
5. Nagase, K.; Kobayashi, J.; Kikuchi, A.; Akiyama, Y.; Kanazawa, H.; Okano. T. *Langmuir* **2008,** *24*, 511.
6. Qiu, J.; Matyjaszewski, K. *Macromolecules* **1997,** *30*, 5463.
7. Zhang, H.; Lei, X.; Su, Z.; Liu, P. J. *Polym. Res.* **2007,** *14*, 253.
8. Hu, B.; Fuchs, A.; Huseyin, S.; Gordaninejad, F.; Evrensel, C. *J. Appl. Polym. Sci.* **2006,** *100*, 2464.
9. Rudnick, L. R. Lubricant Additives; New York: Marcel Dekker, **2003;** Chapter 19.
10. Peale, L. F.; Messina, J.; Ackerman, B.; Sasin, R.; Swern, D. *ASLE Trans.* **1960,** *3*, 48.
11. Park, J. H.; Kwon, M. H.; Park, O. O. *Korean J. Chem. Eng.* **2001,** *18*, 580.
12. Jianqiang, H.; Huanqin, Z.; Li, W.; Xianyong, W.; Feng, J.; Zhiming, Z. *Wear* **2005,** *259*, 519.
13. Rabinow, J. *AIEE Transact.* **1948,** *67*, 1308.
14. Phule, P.; Ginder, J. M. *MRS Bull. Aug* **1998,** 19.
15. Liu, Y.; Gordaninejad, F.; Evrensel, C.; Wang, X.; Hitchcock, G. *ASCE J. Struct. Eng.* **2005,** *131*, 743.
16. Rankin, P. J.; Horvath, A. T.; Klingenberg, D. *J. Rheol. Acta.* **1999,** *38*, 471.
17. Fuchs, A.; Zhang, Q.; Elkins, J.; Gordaninejad, F.; Evrensel, C. *J. Appl. Polym. Sci.* **2007,** *105*, 2497.
18. Elkins, J. Chemical Engineering Master Thesis, University of Nevada, Reno, **2005.**
19. Zhang, Q. Chemical Engineering Master Thesis, University of Nevada, Reno, **2005.**
20. Fuchs, A.; Sutrisno, J.; Gordaninejad, F.; Calgar, M.; Liu, Y. *J. Appl. Polym. Sci.* **2009,** *117*, 934.
21. Ning, Y. C. Structural Identification of Organic Compounds with Spectroscopic Technique. Weinheim: Wiley-VCH, **2005** (appendix 2).
22. Lau, W. S. Infrared Characterization for Microelectronics. Singapore: World Scientific Publishing, **1999;** Chapter 8.
23. Szymanski, H. A. Interpreted Infrared Spectra; New York: Plenum Press, **1964** (alkanes – alkenes section).
24. Silverstein, R. M.; Bassler, G. C. Spectrometric Identification of Organic Compounds; London: Wiley, **1963;** Chapter 3.
25. McMurry, J. Organic Chemistry, 4th ed.; Pacific Grove: Brooks/Cole Pub., **1995.**
26. Nyquist, R. A. Interpreting Infrared, Raman, and Nuclear Magnetic Resonance Spectra; Academic Press: London, **2001** (Table 11.17A).
27. Wang, X.S.; Armes, S. P. *Macromolecules* **2000,** *33*, 6640.
28. Jin, S.; Liu, M.; Chen, S.; Gao, C. *Macromol. Chem. Phys.* **2008,** *209*, 410.
29. Conrad, M. P. C.; Shoichet, M. S. *Polymer* **2007,** *48*, 5233.
30. Sandler, S. R.; Karo, W. Polymer Synthesis Volume I; Academic Press: New York and London, **1974.**
31. Morinaga, T.; Ohkura, M.; Ohno, K.; Tsujii, Y.; Fukuda, T. *Macromolecules* **2007,** *40*, 1159.
32. Zhang, H.; Lei, X.; Su, Z.; Liu, P. J. *Polym. Res.* **2007,** *14*, 253.
33. Vukovic, R.; Karasz, F. E.; Macknight, W. J. *J. Appl. Polym. Sci.* **1983,** *28*, 219.
34. Hu, B.; Fuchs, A.; Huseyin, S.; Gordaninejad, F.; Evrensel, C. *Polymer* **2006,** *47*, 7653.
35. Felt, D. W.; Hagenbuchle, M.; Liu, J.; Richard, J. *J. Intelligent Mater. Syst. Struct.* **1996,** *7*, 589.
36. Martin, J. E.; Odinek, J.; Halsey, T. C.; Kamien, R. *Phys. Rev. E* **1998,** *57*, 756.
37. Huseyin, S.; Wang, X.; Gordaninejad, F. *J. Intelligent Mater. Syst. Struct.* **2009,** *20*, 2215.

38. Li, W. H.; Du, H.; Chen, G.; Yeo, S. H. *Mater. Sci. Eng. A* **2002,** *333*, 68.

39. Bossis, G.; Lacis, S.; Meuniera, A.; Volkova, O. *J. Magnet. Magn. Mater.* **2002,** *252*, 224.

40. Popplewell, J.; Rosensweig, R. E. *J. Phys. D: Appl. Phys.* **1996,** *29*, 2297.

41. Available at: http://www.halocarbon.com/NewsEvents/TechnicalArticles/Fluorine101.php.

42. Souzy, R.; Ameduri, B.; Boutevin, B. *Prog. Polym. Sci.* **2004,** *29*, 75.

43. Smith, D. W., Jr; Babb, D. A.; Shah, H. V.; Hoeglund, A.; Traiphol, R.; Perahia, D.; Boone, H. W.; Langhoff, C.; Radler, M. *J. Fluorine Chem.* **2000,** *104*, 109.

44. Babb, D. A.; Ezzell, B. R.; Clement, K. S.; Richey, W. F.; Kennedy, A. P. *J. Polym. Sci.: Part A Polym. Chem.* **1993,** *31*, 3465.